Available online at www.sciencedirect.com

SciVerse ScienceDirect

Ceramics International 39 (2013) 425–429

CERAMICS INTERNATIONAL

www.elsevier.com/locate/ceramint

Enhanced dielectric and piezoelectric properties in Li/Sb-modified (Na, K)NbO_3 ceramics by optimizing sintering temperature

Yongjie Zhao*, Rongxia Huang, Rongzheng Liu, Xilin Wang, Heping Zhou

State Key Laboratory of New Ceramics and Fine Processing, Department of Materials Science and Engineering, Tsinghua University, Beijing 100084, PR China

Received 10 May 2012; received in revised form 14 June 2012; accepted 14 June 2012
Available online 21 June 2012

Abstract

In this paper, lead-free $(Na_{0.474}K_{0.474}Li_{0.052})(Nb_{0.948}Sb_{0.052})O_3$ ceramics were synthesized by a conventional solid-state reaction route. The effects of sintering temperature on the crystal structure, microstructure, densification, dielectric properties, and ferroelectric properties of the KNNLS ceramics were addressed. X-ray diffraction patterns and Raman spectrum indicated a transition from orthorhombic to tetragonal phase during the sintering temperature region. This transition is attributed to the migration of Li between the matrix grain and grain boundary. Scanning electron microscopy study revealed increased grain size and enhanced densification with increasing sintering temperature. The density of the ceramics sintered at 1080 °C reached a maximum value of 4.22 g/cm^3. KNNLS ceramics sintered at an optimum temperature of 1080 °C exhibited high piezoelectric properties, that is 242 pC/N for d_{33}, 0.42 for k_p and 18.2 μC/cm^2 for P_r.

Keywords: A. Ceramics; B. Chemical synthesis; B. X-ray diffraction; D. Piezoelectricity

1. Introduction

It is known that the temperature dependent piezoelectric properties (polymorphism phase transition) strongly restrict the use of KNN-based ceramics. Studies indicate that the cubic–tetragonal phase transition and the tetragonal–orthorhombic phase transition are restrained by the substitution of Sb^{5+} for Nb^{5+}, and which also induces the temperature independent piezoelectric properties over a wide temperature range [1–4]. Therefore, the temperature stability of KNN-based ceramics was greatly improved, and Sb especially Li/Sb-modified KNN ceramics become very attractive lead-free materials for the applications in devices like transducer, sensor and so forth. So lots of efforts were emphasized on the relating research of this system.

Most properties of piezoelectric ceramics, such as dielectric, ferroelectric, and piezoelectric properties, strongly depend on the sintering temperature. The high d_{33} coefficient reached 265 pC/N, which was obtained with a nominal MPB-like composition of Li/Sb-modified KNN ceramics [4]. This strong piezoelectric property is attributed to the following two factors: one is the coexistence of orthorhombic and tetragonal phase; the other is the precisely controlled amount of Na and K volatilized, achieved by optimizing the sintering temperature. Concerning with KNN based ceramics, the volatilization of alkali metal elements usually occurs; however, a sufficiently high sintering temperature is required to obtain dense microstructures. Thus, optimization of sintering parameters is important not only for densification but also for controlling composition of the ceramics [5–7]. The change of phase structure and the deviation of composition have considerably effect on the performance of various electrical properties [8–9]. The volatilization of alkali-metal elements may not be the only factor for the phase change of alkaline niobate-based ceramics. Wang's research proved that the phase change of KNN-based ceramics induced by varying the sintering temperature, which resulted from the volatilization and segregation of the alkali metal elements [10]. So the phase change with the

*Corresponding author. Tel.: +86 10 62772549; fax: +86 10 62772549.
E-mail address: zhaoyjpeace@gmail.com (Y. Zhao).

0272-8842/$36.00
http://dx.doi.org/10.1016/j.ceramint.2012.06.043

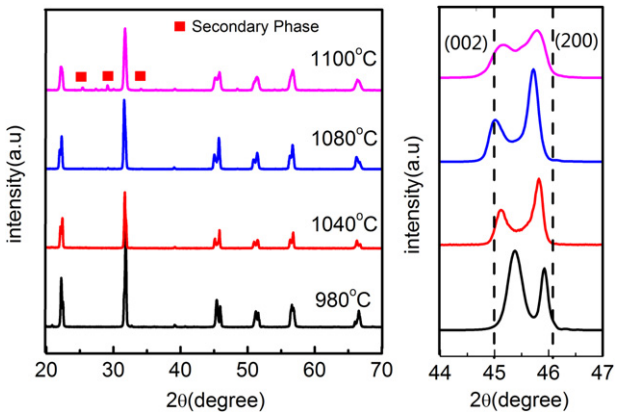

Fig. 1. XRD patterns and expanded XRD patterns in the range 44–47°.

sintering temperature could not simply be attributed to the volatilization. Elaborately controlling the sintering temperature is the essence to the high performance KNN-based piezoelectric ceramics.

In fact, as the solution of Li in the matrix is very important for the room temperature of Li-modified KNN ceramics, the microstructure and electrical properties of the Li/Sb-codoped KNN ceramics are more sensitive to the sintering temperature than those of the Li-free KNN ceramics. This study mainly focused on the effects of sintering temperature on the microstructure characteristic, phase structure and electrical properties of $K_{0.5}Na_{0.5}NbO_3$–$LiSbO_3$ ceramics. Through optimizing the compensating amount of Na and K at a fixed and optimized ratio of 0.5:0.5, $(Na_{0.474}K_{0.474}Li_{0.052})(Nb_{0.948}Sb_{0.052})O_3$ (KKNLNS) was determined as the optimal composition for the Li/Sb-codoped KNN system.

2. Experimental

Lead free $(Na_{0.474}K_{0.474}Li_{0.052})(Nb_{0.948}Sb_{0.052})O_3$ (KNNLS) ceramics were prepared by a conventional solid state reaction route. Sodium carbonate (Na_2CO_3, 99% purity), potassium carbonate (K_2CO_3, 99% purity), lithium carbonate (Li_2CO_3, 99% purity), niobium pentoxide (Nb_2O_5, 99% purity) and antimony trioxide (Sb_2O_3, 99% purity) were used as starting materials. Stoichiometric weights of all the powders were mixed and ball milled with acetone for 24 h, using zirconia balls as the grinding media. After drying the slurry in oven, the calcination was carried out at 750 °C for 6 h in air. The calcined powder was mixed thoroughly with polyvinyl butyral (PVB) binder solution and then pressed into disks of diameter of 10 mm and a thickness of 1 mm under 60 MPa pressure.

The sintering of the samples was carried out at 980, 1040, 1080 and 1100 °C for 2 h in air, respectively. XRD analysis of the pellets was performed on X-ray powder diffraction (D/MAX-2500, Rigaku, Tokyo, Japan) with a $CuK\alpha_1$ radiation ($\lambda = 0.15406$ nm) in order to examine the phases structure. The sintered microstructures were observed using scanning electron microscopy (SEM, LEO-1530, Oberkochen, Germany). The bulk densities of the samples were measured by the Archimedes method. Silver paste was applied on both sides of the samples for the electrical measurements. The planar electromechanical coupling factor k_p were determined by the resonance–antiresonance method according to IEEE standards using an impedance analyzer (HP 4194A). Dielectric constant and dielectric loss were measured using a LCR meter (TH2816, China) at 1 kHz. Raman scattering was excited using the 633 nm radiation from He–Ne laser and was collected by a micro-Raman spectrometer (HORIBA Jobin Yvon) in the 100–1000 cm^{-1} range at room temperature.

3. Results and discussion

Fig. 1 shows the room temperature X-ray diffraction patterns of KNNLS samples sintered at different temperatures. The XRD peaks are found to be sharp and distinct indicating good homogeneity and crystallinity of the samples. There are obvious differences among these XRD patterns, which indicate that a transition from orthorhombic to tetragonal phase occurs in the samples sintered at 980–1100 °C. In previous studies [11,12], this kind of temperature dependence of phase structure transition behavior was also found, and this behavior was attributed to the different extents of the volatilization of alkali metal ions during sintering at different temperatures.

The samples sintered at 980 °C possesses orthorhombic phase while the samples for 1040 °C is tetragonal phase. It is reported that the migration of Li between the matrix grains and grain boundaries during sintering is responsible for the drastic variation of the phase structure [10]. So we consider that when the sintering temperature is below 1040 °C, the Li converges along the grain boundaries, and XRD pattern just represents the phase of matrix grain (K:Na = 1:1). However, as chemical analysis techniques used here could not detect Li element, we cannot directly confirm this point.

Single perovskite phase is developed at the sintering temperature of 980, 1040 and 1080 °C, whereas at the temperature of 1100 °C secondary phase along with the perovskite phase is developed in KNNLS samples. The development of secondary phase may be due to the evaporation of alkali metal. The diffraction peaks slightly shift to a lower angle with increasing sintering temperature as shown in Fig. 1. The slightly increased space distance is caused by the following reasons. At high temperature, both Na and K are volatile but Na is more serious. With increasing sintering temperature, the heavier loss of Na makes the K content relatively higher in the sample. Moreover, the larger radius of K (1.33 Å) than that of Na (0.97 Å) give rise to the eventually increased crystal parameters.

The Raman spectra of the sintered samples present the typical vibrations corresponding to a perovskite phase. A detail of the region between 100 and 1000 cm^{-1} of KNNLS sintered at various temperatures and the powders calcined at 760 °C are presented in Fig. 2. The peak v_2 and v_5 shifts to higher wavenumbers with the sintering

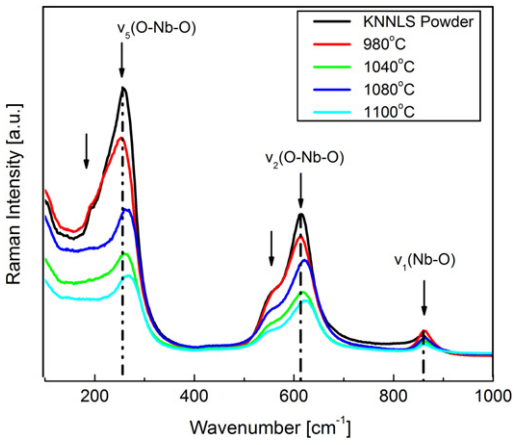

Fig. 2. Room temperature Raman spectra of the KNNLS ceramics sintered at various temperatures and KNNLS powder calcined at 760 °C.

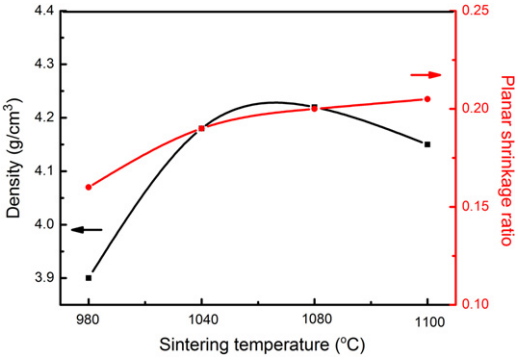

Fig. 3. Variation of density and planar shrinkage ratio of KNNLS ceramics sintered at various temperatures.

temperature increasing due to an increase in the force constant, caused by the shortening of the distance between B^{5+} type ions and their coordinated oxygen. The same evolution was observed in KNL-NTS [13]. The main essence of Raman result is the observation of a shift in the crystal symmetry of the perovskite phase from orthorhombic to tetragonal symmetry with the increase of sintering temperature. In modified-KNN and related systems, the tetragonal to orthorhombic phase transition shifts toward lower temperatures when the concentration of Li^+ increases [14,15]. The result to some extent supports the point that the migration of Li during sintering is responsible for the drastic variation of the phase structure.

Fig. 3 shows the change of the density and planar shrinkage ratio of KNNLS samples as a function of sintering temperature. Note that the density changed significantly within a narrow range. The density of the KNNLS samples increased from 3.9 to 4.22 g/cm^3 when the sintering temperature was increased by a scope of 100 °C from 980 °C to 1080 °C, but it tended to decrease when the temperature was further increased. At the same time, it was observed that the planar shrinkage ratio increased obviously with the increase of sintering temperature to a higher value of 0.2 at 1080 °C. However, the parameters slightly fluctuated as the sintering temperature increased up to 1100 °C. It indicates that the dense KNNLS ceramics could be obtained at the sintering temperature above 1080 °C.

Fig. 4 shows SEM images of the fracture of KNNLS ceramics sintered at different temperatures. The as sintered surface of the samples could not represent the bulk on account of the volatilization of alkali metal. Therefore, the fracture of the as sintered ceramics was employed. As shown in Fig. 4, except for distinct pores observed in the samples sintered at 980 °C, all of the samples possess highly dense microstructure at the sintering temperature between 1040 °C and 1100 °C. In addition, some larger grains (about 10 μm) formed for the samples sintered above 1040 °C. It is considered that the formation of large grains is attributed to the liquid phase, which is consistent with the other reports that the formation of large grains is ascribed to the existence of the liquid phase in the KNN-based ceramics [11].

Fig. 5 shows the d_{33}, k_p, dielectric constant and loss as a function of sintering temperature for the KNNLS ceramics sintered at 980–1100 °C. The variations of the d_{33} and k_p with sintering temperature was closely related with the microstructure. Therefore, the increase of the d_{33} and k_p of specimens with the increasing sintering temperature is resulted from the enhancement of the compact degree and the increase of the grain size of samples. At 1080 °C, d_{33} and k_p reached their maximum values, being 242 pC/N and 0.42, respectively. When the sintering temperature was over 1080 °C, both d_{33} and k_p tend to decrease, which lied in the compositional deviation from the optimal one caused by the heavier losses of Na and K at higher sintering temperatures. The variation of the dielectric constant with sintering temperature is very similar to those of the d_{33} and k_p, the dielectric constant increases with the increasing sintering temperature firstly and then decreases. This is because the grain size increases with the increase of the sintering temperature, which leads to a reduction of the number of the grain boundary.

In order to study the effect of the sintering temperature on the ferroelectric properties, the P–E hysteresis loops of the KNNLS ceramics as a function of the sintering temperature were measured at room temperature. Fig. 6 shows the P–E hysteresis loops of KNNLS with different sintering temperatures, while the variations of the remnant polarization P_r and coercive field E_c with sintering temperature are also showed in Fig. 6. It is clearly observed that the shapes of P–E loop greatly vary with the sintering temperature. The P–E loops of the samples sintered at 1040 °C and 1080 °C are well developed. A maximum remnant polarization (P_r=18.2 μC/cm^2) and low coercive field (E_c=1.4 kV/mm) were obtained when the sintering temperature was 1080 °C. The increase in P_r for the KNNLS sample sintered at 1080 °C can be associated with the increase in domain wall motion with the increase in grain size which helps in switching the domains and hence affects the polarization. The decrease of P_r at 1100 °C may be due to the non-uniform grain size, evaporation of

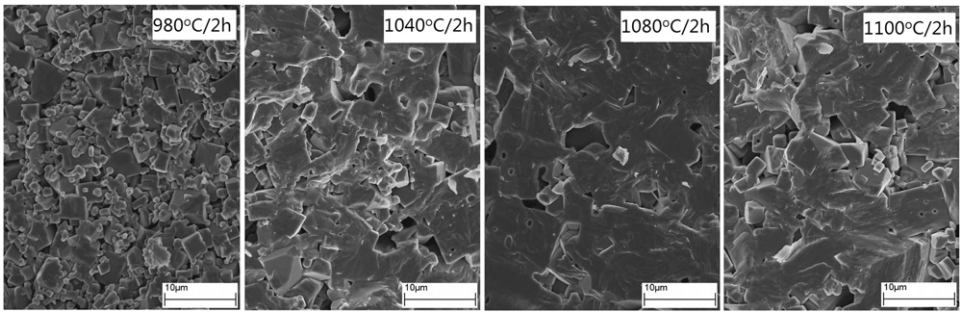

Fig. 4. Scanning electron microscopic micrograph of the fracture of the as sintered KNNLS samples.

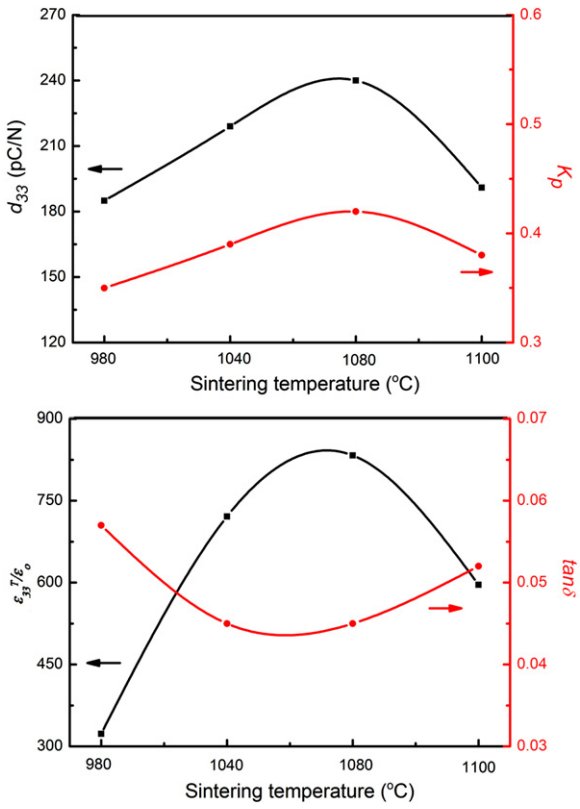

Fig. 5. Piezoelectric and dielectric properties of the KNNLS ceramics with different sintering temperatures.

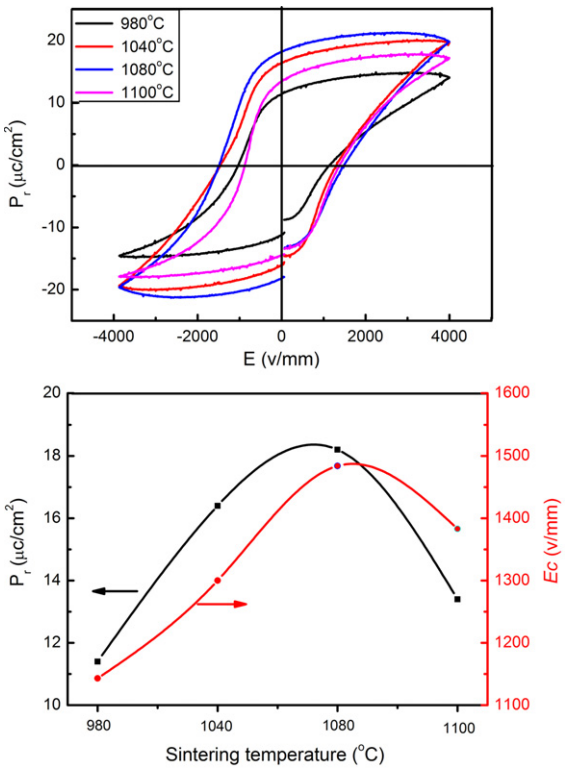

Fig. 6. Polarization-electric field hysteresis loops of KNNLS ceramics sintered at four temperature points.

potassium oxide and development of non-ferroelectric secondary phase. Taking the above result into consideration, it could be concluded that the optimum sintering temperature for KNNLS should be 1080 °C.

4. Conclusions

Lead-free KNNLS piezoelectric ceramics are prepared by the conventional solid state reaction and normal sintering processes. The effects of the sintering temperature on the crystallographic structure, microstructure and electrical properties, were investigated. This work provides us with guidance concerning the preparation of high performance KNNLS based piezoelectric ceramics. Through optimizing sintering temperature, the grain growth, densification and the ferroelectric properties were enhanced. The samples sintered at 1080 °C showed dense microstructure and good ferroelectric properties. The piezoelectric constant d_{33} of 242 pC/N, planar electromechanical coupling factor k_p of 0.42, remnant polarization P_r of 18.2 μC/cm^2 and coercive field E_c of 1.4 kV/mm was obtained at this optimum temperature.

Acknowledgments

This work was supported by the National Natural Science Foundation of China.

References

[1] D.M. Lin, K.W. Kwok, H.L.W. Chan, Phase transitions and electrical properties of $(Na_{1-x}K_x)(Nb_{1-y}Sb_y)O_3$ lead-free piezoelectric ceramics with a MnO_2 sintering aid, Journal of the American Ceramic Society 90 (2007) 1458.

[2] Y.F Chang, Z.P Yang, Y.T. Hou, Z.H Liu, Z.L. Wang, Effects of Li content on the phase structure and electrical properties of lead-free $(K_{[0.46-x/2]}Na_{[0.54-x/2]}Li_x)(Nb_{0.76}Ta_{0.20}Sb_{0.04})O_3$ ceramics, Applied Physics Letters 90 (2007) 232905.

[3] Y.F Chang, S.F Poterala, Z.P Yang, S. Trolier-McKinstry, G.L. Messing, (001) textured (K0.5Na0.5)(Nb0.97Sb0.03)O3 piezoelectric ceramics with high electromechanical coupling over a broad temperature range, Applied Physics Letters 95 (2009) 232905.

[4] S.J. Zhang, R. Xia, T.R. Shrout, G.Z. Zang, J.F. Wang, Piezoelectric properties in perovskite $0.948(K_{0.5}Na_{0.5})NbO_3$–$0.052LiSbO_3$ lead-free ceramics, Journal of Applied Physics 100 (2006) 104108.

[5] R.C. Chang, S.Y. Chu, Y.P. Wong, C.S. Hong, H.H. Huang, The effects of sintering temperature on the properties of lead-free $(Na_{0.5}K_{0.5})NbO_3$–$SrTiO_3$ ceramics, Journal of Alloys and Compounds 456 (2008) 308.

[6] M.R. Yang, C.S. Hong, C.C. Tsai, S.Y. Chu, Effect of sintering temperature on the piezoelectric and ferroelectric characteristics of CuO doped $0.95(Na_{0.5}K_{0.5})NbO_3$–$0.05LiTaO_3$ ceramics, Journal of Alloys and Compounds 488 (2009) 169.

[7] Y.J. Zhao, Y.Z. Zhao, R.X. Huang, R.Z. Liu, H.P. Zhou, Effect of sintering temperature on microstructure and electric properties of $0.95(K_{0.5}Na_{0.5})NbO_3$–$0.05Li(Nb_{0.5}Sb_{0.5})O_3$with copper oxide sintering aid, Journal of the American Ceramic Society 94 (2011) 656.

[8] J.G. Wu, D.Q. Xiao, Y.Y. Wang, J.G. Zhu, W. Shi, W.J. Wu, B. Zhang, J. Lia, Phase structure, microstructure and ferroelectric properties of $(1-x)[(K_{0.50}Na_{0.50})_{0.94}Li_{0.06}](Nb_{0.94}Sb_{0.06})O_3-xCaTiO_3$ lead-free ceramics, Journal of Alloys and Compounds 476 (2009) 782.

[9] K.C. Singh, C. Jiten, R. Laishram, O.P. Thakur, D.K. Bhattacharya, Structure and electrical properties of Li- and Ta-substituted $K_{0.5}Na_{0.5}NbO_3$ lead-free piezoelectric ceramics prepared from nanopowders, Journal of Alloys and Compounds 496 (2010) 717.

[10] Y.L. Wang, D. Damjanovic, N. Klein, High-temperature instability of Li- and Ta-modified (K, Na)NbO_3 piezoceramics, Journal of the American Ceramic Society 91 (2008) 1962.

[11] Y. Zhen, J.F. Li, Normal sintering of (K, Na)NbO_3-based ceramics: influence of sintering temperature on densification, microstructure, and electrical properties, Journal of the American Ceramic Society 89 (2006) 3669.

[12] P. Zhao, B.P. Zhang, J.F. Li, High piezoelectric d_{33} coefficient in Li-modified lead-free (Na, K)NbO_3 ceramics sintered at optimal temperature, Applied Physics Letters 90 (2007) 242909.

[13] F. Rubio-Marcos, M.A. Banares, J.J. Romero, J.F. Fernandez, Correlation between the piezoelectric properties and the structure of lead-free KNN-modified ceramics, studied by Raman Spectroscopy, Journal of Raman Spectroscopy 42 (2011) 639.

[14] K. Kakimoto, K. Akao, Y. Guo, H. Ohsato, Raman scattering study of piezoelectric $(Na_{0.5}K_{0.5})NbO_3$–$LiNbO_3$ ceramics, Japanese Journal of Applied Physics 44 (2005) 7064.

[15] Y. Wang, D. Damjanovic, N. Klein, E. Hollenstein, N. Setter, Compositional inhomogeneity in Li- and Ta-modified (K, Na)NbO_3 Ceramics, Journal of the American Ceramic Society 90 (2007) 3485.